Finite element elasto-plastic analysis of axisymmetric structures by paralinear and other two dimensional elements

T.Kant & J.T.Galagali
Department of Civil Engineering, Indian Institute of Technology, Powai, Bombay, India

1 INTRODUCTION

Lessons learnt from the recent Chernobyl and the Three Mile Island Nuclear disasters have further emphasised the need for greater precision and detail in the analysis of nuclear containments. Though under normal working conditions the behaviour is elastic there is always a non-zero probability of a radioactive leakage, in the even of which the containment walls would be subjected to excessive overpressures. The evaluation of the ultimate load carrying capacity by considering the behaviour in the non-linear range is of paramount importance in the safety assessment of nuclear power plant facilities. However a rigorous non-linear analysis may often be discouraging in view of the enormous computing costs. Such being the case it would seem natural to seek means for performing the analysis economically without sacrificing accuracy.

The type of discretisation employed has a marked influence on the correctness and convergence of the results. Sharma et al. (1983) and Mc Gaughy et al. (1983) used isoparametric quadrilateral elements for the non-linear finite element analyses of Reinforced Concrete Mark III containment. Khatua et al. (1979), Larkin et al. (1979) and Clauss and Horschel (1985) used the degenerate shell element. The elements employed by Zudans (1970), Abel and Wu (1979) and Steel et al. (1979) were based on the shell theory. Rashid and Rockenhouser (1968), Wade and Henrywood (1975), Takeda and Imoto (1975) and Yamaura (1985) used a more detailed 3 D finite element model for the non-linear analysis. Daye and Mayers (1985) employed close form relations for the evaluation of BWR and PWR containment structures subjected to internal pressure.

The present work is an effort made to achieve economy in the discretisation of the structure. The performance of the 6 noded quadratic-linear (paralinear) element as regards its ability to model thin/moderately thick axisymmetric structures, is compared with that of the 4, 8 and 9 noded plane quadrilateral isoparametric elements. Four examples of axisymmetric structures, drawn from literature are presented. Parametric study for different radius/thickness ratios is done using 4, 8, 9 and 6 noded elements. Finally the elasto-plastic analysis of a pressure vessel is done using the different elements.

2 ELASTO-PLASTIC STRESS-STRAIN RELATION

Since in an axisymmetric structure under axisymmetric loads each meridional section will undergo identical deformations there will be no deformation in the circumferential direction. Taking the y axis as the axis of revolution and x axis as the radial direction (Fig. 1) the axisymmetric strains are given by

$$(1) \qquad \underset{\sim}{\varepsilon} = [\varepsilon_x, \varepsilon_y, \gamma_{xy}, \varepsilon_\theta]^T = [\partial u/\partial x,\ \partial v/\partial y,\ \partial u/\partial y + \partial v/\partial x,\ u/x]^T$$

where ε_x = strain in the radial direction

ε_y = strain in the axial direction;

γ_{xy} = shear strain in the meridional plane

ε_θ = strain in circumferential direction

u,v = displacements in x and y direction respectively.

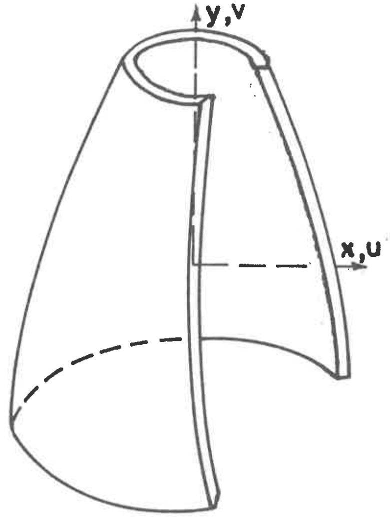

Fig. 1

The stresses are given by

$$(2) \qquad \underset{\sim}{\sigma} = [\sigma_x, \sigma_y, \tau_{xy}, \sigma_\theta]^T = \underline{D}_{ep} \underset{\sim}{\varepsilon}$$

where σ_x = stress in the radial direction;

σ_y = stress in the axial direction;

τ_{xy} = shear stress in the meridional plane;

σ_θ = stress in the circumferential direction.

$$(3) \qquad \underline{D}_{ep} = \underline{D} - \frac{\underset{\sim}{d}_D\, \underset{\sim}{d}_D^T}{A + \underset{\sim}{d}^T \underset{\sim}{a}}$$

$$(4) \qquad d_D = \underline{D}\, \underset{\sim}{a}$$

$$(5) \qquad \underline{D} = \frac{E(1-\nu)}{(1+\nu)(1-\nu)} \begin{bmatrix} 1 & \frac{\nu}{1-\nu} & 0 & \frac{\nu}{1-\nu} \\ & 1 & 0 & \frac{\nu}{1-\nu} \\ & & \frac{1-2\nu}{2(1-\nu)} & 0 \\ \text{SYMMETRIC} & & & 1 \end{bmatrix}$$

where E = Youngs modulus and ν = Poisons ratio.

$\underset{\sim}{a}$ is the flow vector given by

$$(6) \qquad \underset{\sim}{a}^T = [\partial F/\partial\sigma_x,\ \partial F/\partial\sigma_y,\ \partial F/\partial\tau_{xy},\ \partial F/\partial\sigma_\theta]$$

and F is the relevant yield function and A is the strain hardening parameter.

3 FINITE ELEMENT DISCRETISATION

We follow the standard finite element discretisation procedure in which the total solution domain Ω is sub-divided into 'ME' sub-domains (elements) $\Omega_1, \Omega_2, \ldots, \Omega_{ME}$ such that,

$$(7) \qquad \Pi(\underset{\sim}{d}) = \sum_{1}^{ME} \Pi^e(\underset{\sim}{d})$$

where Π and Π^e are the total potential of the system and element respectively. We further express,

$$(8) \qquad \Pi^e(\underset{\sim}{d}) = U^e - W^e$$

in which U^e and W^e are the internal strain energy and the external work done expressions respectively and $\underset{\sim}{d}$ is the vector of displacement variables in the problem and is defined in the present case as :

$$(9) \qquad \underset{\sim}{d} = (u, v)^T$$

In the C^0 finite element theory the continuum displacement vector within the element is discretised such that,

$$(10) \qquad \underset{\sim}{d} = \sum_{1}^{NE} N_i(x, y)\, \underset{\sim}{d}_i$$

in which $N_i(x,y)$ is the interpolating (shape) function associated with node i, $\underset{\sim}{d}_i$ is the value of $\underset{\sim}{d}$ corresponding to node i and 'NE' is the number of nodes in the element.

In the present analyses, the 6, 4, 8 and 9 noded isoparametric ring elements with two degrees of freedom per node as per equation (9) are used. With the generalised displacement vector $\underset{\sim}{d}$ known at all points within the element as per equation (10), the generalised strain vector $\underset{\sim}{\varepsilon}$ at any point is expressed as

$$(11) \qquad \underset{\sim}{\varepsilon} = \sum_{i=1}^{NE} \begin{bmatrix} \frac{\partial N_i}{\partial x} & 0 \\ 0 & \frac{\partial N_i}{\partial y} \\ \frac{\partial N_i}{\partial y} & \frac{\partial N_i}{\partial x} \\ \frac{N_i}{x} & 0 \end{bmatrix} \begin{Bmatrix} u_i \\ v_i \end{Bmatrix}$$

$$(12) \quad \text{Or} \qquad \underset{\sim}{\varepsilon} = \sum_{i=1}^{NE} \underset{\sim}{B}_i\, \underset{\sim}{d}_i$$

In computing the stiffness of matrix the integration has to be carried out over the volume of the ring element, i.e., integration in x, y and 0. Since all terms with rrspect to 0 are constants this involves area integration multiplied by 2 x. Thus

$$(13) \qquad \underset{\sim}{K} = \iint \underset{\sim}{B}^T D_{ep}\, \underset{\sim}{B}\, 2\pi x \, dx\, dy$$

$$(14) \qquad = \sum_{1}^{NG} \sum_{1}^{NG} \underset{\sim}{B}^T(\xi_i, \eta_i)\, \underset{\sim}{D}_{ep}\, \underset{\sim}{B}(\xi_i, \eta_i) \det |J \ (\xi_i, \eta_i)|\ 2\pi x$$

where NG denotes the order of integration.

The consistent nodal forces for node i can be shown to be

$$P_{xi}^{(e)} = \int_{\Gamma^{(e)}} N_i^{(e)} \left(p_t \frac{\partial x}{\partial \xi} - p_n \frac{\partial y}{\partial \xi}\right) d\xi \; ; \quad P_{yi}^{(e)} = \int_{\Gamma^{(e)}} N_i^{(e)} \left(p_t \frac{\partial x}{\partial \xi} + p_t \frac{\partial y}{\partial \xi}\right) d\xi$$

where p_n and p_t are the normal and tangential distributed loads respectively. Integration is taken along the loaded element edge $\Gamma^{(e)}$

4 THIN AXISYMMETRIC STRUCTURES

When thin shell structures are modelled by the 6 noded paralinear element two conditions are to be met with viz., inextensibility of the middle plane in bending and zero normal stress. In order to meet these requirements the elasticity matrix is modified by decoupling the longitudinal stresses and strains from the other stresses and strains and by setting the second row and column of the elasticity matrix to zero.

However due to the thinness of the structure the stiffness coefficients connecting opposite nodes are much higher than the other terms. This results in the illconditioning of the stiffness matrix which leads to large roundoff errors. These errors become serious when the aspect ratio exceeds about ten. In order to circumvent this problem, the nodal displacements of one face are expressed as differential displacements with respect to the opposite face. Refering to Fig. 2, we have

$$(15) \quad \left[d_1^*, d_2^*, d_3^*, d_4^*, d_5^*, d_6^*\right]^T = \left[d_1 - d_6, d_2 - d_5, d_3 - d_4, d_4, d_5, d_6\right]^T$$

the shape functions are modified so as to be compatible with the differential displacements.

$$(16) \quad N_1^* = N_1; \; N_2^* = N_2; \; N_3^* = N_3;$$
$$N_4^* = N_3 + N_4; \; N_5^* = N_2 + N_5$$
$$N_6^* = N_1 + N_6$$

The $\underline{B}$ matrix is modified as,

$$(17) \quad \underline{B}^* = \left[\underline{B}_1 \vdots \underline{B}_2 \vdots \underline{B}_3 \vdots \underline{B}_4 + \underline{B}_3 \vdots \underline{B}_5 + \underline{B}_2 \vdots \underline{B}_6 + \underline{B}_1\right]$$

$$(18) \text{ and } \underline{B}_i = \begin{bmatrix} \dfrac{\partial N_i}{\partial x} & 0 & \dfrac{\partial N_i}{\partial y} & \dfrac{N_i}{x} \\ 0 & \dfrac{\partial N_i}{\partial y} & \dfrac{\partial N_i}{\partial x} & 0 \end{bmatrix}^T$$

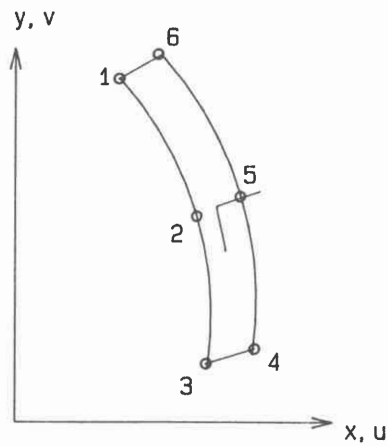

Fig. 2

The strain vector which is formed in the local axes is expressible in terms of the global degrees of freedom by the following transformation and the stresses are given by equations (19) and (20) respectively.

$$(19)\quad \underset{\sim}{\varepsilon} = \begin{Bmatrix} \varepsilon'_x \\ \varepsilon'_y \\ \gamma'_{xy} \\ \varepsilon'_\theta \end{Bmatrix} = \begin{bmatrix} \frac{\partial u'}{\partial x'} \\ \frac{\partial v'}{\partial y'} \\ \frac{\partial u'}{\partial y'} + \frac{\partial u'}{\partial x'} \\ \frac{u'}{x'} \end{bmatrix} = \underline{T} \begin{bmatrix} \frac{\partial u}{\partial x} \\ \frac{\partial v}{\partial y} \\ \frac{\partial u}{\partial y} + \frac{\partial v}{\partial x} \\ \frac{u}{x} \end{bmatrix} = \underline{T}\,\underline{B}\,\underset{\sim}{d} = \underline{B}'\,\underset{\sim}{d}$$

$$(20)\quad \underset{\sim}{\sigma}' = \left[\sigma'_x,\ \sigma'_y,\ \tau'_{xy},\ \sigma'_\theta\right]^T = \underline{D}_{ep}\,\underset{\sim}{\varepsilon}'$$

where $\underset{\sim}{\varepsilon}'$ and $\underset{\sim}{\sigma}'$ are the strain and stress vectors in the local x' and y' axes respectively; u' and v' are the displacements along the local x' and y' axes respectively; $\underline{B}'$ represents the transformed B matrix. The transformation matrix $\underline{T}$ is given by

$$(21)\quad \underline{T} = \begin{bmatrix} l_1^2 & m_1^2 & l_1 m_1 & 0 \\ l_2^2 & m_2^2 & l_2 m_2 & 0 \\ 2 l_1 l_2 & 2 m_1 m_2 & l_2 m_1 + m_1 l_2 & 0 \\ 0 & 0 & 0 & 1 \end{bmatrix} \quad \text{where} \quad l_1 = \frac{\partial x}{\partial \xi};\quad l_2 = \frac{\partial x}{\partial \eta};\quad m_1 = \frac{\partial y}{\partial \xi};\quad m_2 = \frac{\partial x}{\partial \eta}$$

5 RESULTS AND CONCLUSIONS

Example-1: The first example (Fig. 3) is the simple case of an infinitely long cylinder. The geometric and material properties are lnegth L = 2", thickness h = 0.03"; radius r = 3"; Youngs modulus $E = 30 \times 10^6$ psi and Poison's ratio =0.3. This gives an r/h of 100 and differential displacements are used for the paralinear element. Results tabulated in Fig. 4 show close agreement with the analytical solution given by Timoshenko (1970).

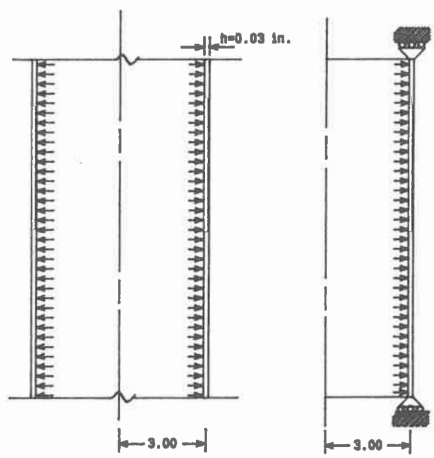

Fig. 3

Example-2: This example taken from Kant (1976) and Baluch (1970) is that of a circular cylindrical shell subject to unit transverse shear at the free edge and clamped at the other edge (Fig. 5). The geometrical and material properties are, length L = 25"; radius r = 10"; Youngs modulus $E = 30 \times 10^6$ psi; Poison ratio =0.3.

Parametric study is done for 4, 8, 9 and 6 noded elements and h is varied so as to obtain r/h ratio as 4, 5, 10, 15 and 20. Results presented in Fig. 6 clearly show close agreement of the 6 noded paralinear element with that of Kant (1976).

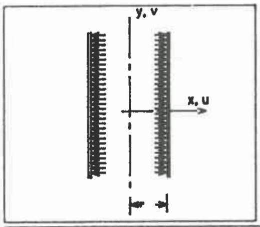

analytical solution
deflection u = 1.0 X 10^{-4} in.
hoop stress = 100.00 psi

fem solution				
no. of nodes per element	no. of elements	aspect ratio	u deflection X 10^{-4} in.	hoop stress psi
6	1	66.67	0.990	95.50
4	16	4.17	1.210	108.90
8	8	8.33	0.989	99.23
9	8	8.33	0.987	98.98

Fig. 4

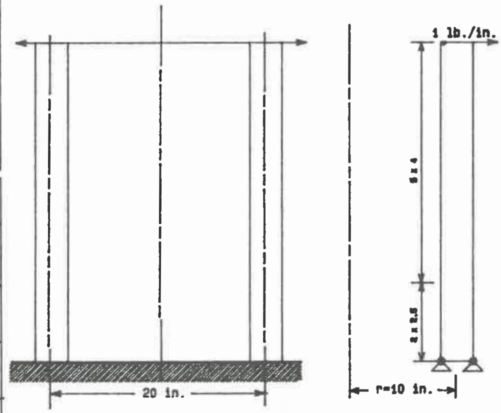

Fig. 5

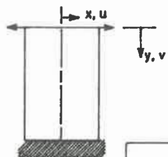

r/h	y	NO. OF NODES PER ELEMENT 6	4	8	9	KANT
4	0	66.7	55.6	74.55	91.56	69.44
	2	33.97	27.50	36.58	28.12	33.33
	4	12.10	11.19	12.08	27.98	11.11
	6	-4.17	-3.12	2.56	-7.41	-3.10
5	0	95.50	87.09	102.30	115.31	100.00
	2	44.90	43.32	46.12	39.68	44.44
	4	12.13	14.05	11.61	23.84	11.11
	6	-2.32	-8.39	-3.03	-8.82	-2.78
10	0	266.06	208.96	281.95	285.27	275.00
	2	86.10	87.15	81.68	82.24	80.56
	4	-3.43	14.28	-1.29	-1.53	-3.00
	6	-18.67	-12.92	-18.13	-21.89	-16.67
15	0	481.20	333.32	506.68	511.50	500.00
	2	111.11	128.88	106.45	103.96	88.88
	4	-34.01	12.56	-38.81	-32.20	27.77
	6	-27.67	-24.37	-27.10	-27.09	25.00

(values of deflection u in inches)

Fig. 6

Example-3: The third example taken from Kant (1976) and Goldberg et al. (1975) is that of an axisymmetric container in the form of a circular cylinder built-in at both edges and subjected to an internal pressure of 1 kg/cm2 (Fig. 8). The geometric and material properties are radius r = 200 cm length L = 800 cm, Youngs modulus $E = 2.1 \times 10^5$ kg/cm2 and Poisons ratio = 0.1

The parametric study for r/h = 5, 10, 15 and 20 with 4, 8, 9 and 6 noded elements is done. Results tabulated in Fig. 9 show excellent comparison with those obtained by Kant (1976).

Example-4: In the last example (Fig.11) taken from Zudans (1970), the elasto-plastic analysis of a pressure vessel subjected to uniform internal pressure is done. The material properties assumed are Youngs modulus $E = 30 \times 10^6$ psi; Poisons ratio = 0.3; uniaxial yield strength $\sigma_y^o = 55 \times 10^5$ psi and hardening parameter H' = 0. 4, 8, 9 and 6 noded elements are used. The details are given in Table 1.

After initial yielding, increments of 6 psi were applied till the structure failed. Significant plasticity is observed near the knuckle region. The deflected profile at 40 psi is shown in Fig. 13. The load deflection curve is plotted in Fig. 12.

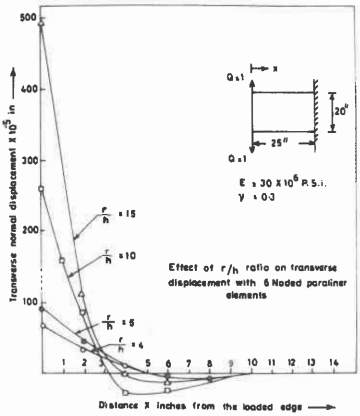

FIG. 5.123 EFFECT OF r/h ON TRANSVERSE NORMAL DISPLACEMENT

Fig. 7

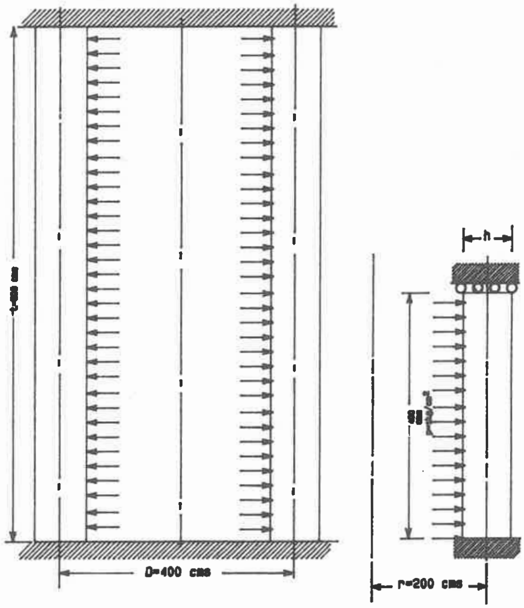

Fig. 8

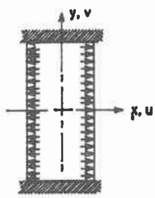

	NO. OF NODES PER ELEMENT				
r/h	6	4	8	9	KANT
05	0.00452	0.00568	0.00454	0.00455	0.00488
10	0.00944	0.01120	0.00946	0.00940	0.00981
15	0.01440	0.01911	0.01438	0.01439	0.01473
20	0.01928	0.02577	0.01928	0.01925	0.01962

(max. u displacement - cms)

Fig. 9

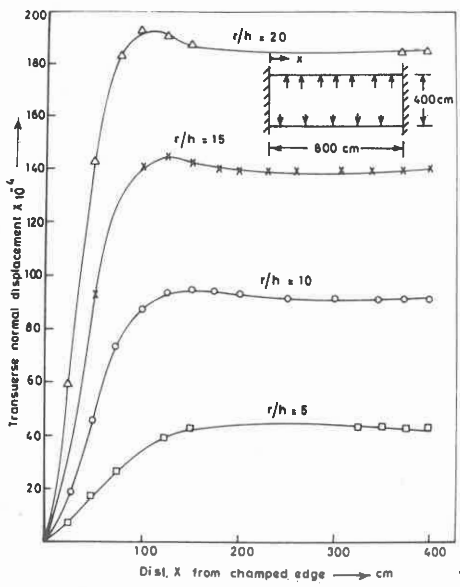

FIG. 5.133 EFFECT OF r/h ON TRANSVERSE NORMAL DESPLACEMENT

Fig. 10

With the use of 4 noded elements the CPU time increased because of the more number of elements. The convergence was uncertain with each increment of load requiring significantly more number of iterations. However with 6, 8 and 9 noded elements the convergence was observed to be uniformly steady. The discretisation with 8 and 9 noded elements near identical values of deflections and stresses are obtained. The

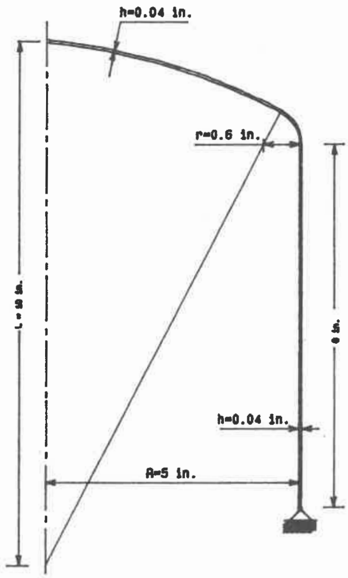

Fig. 11

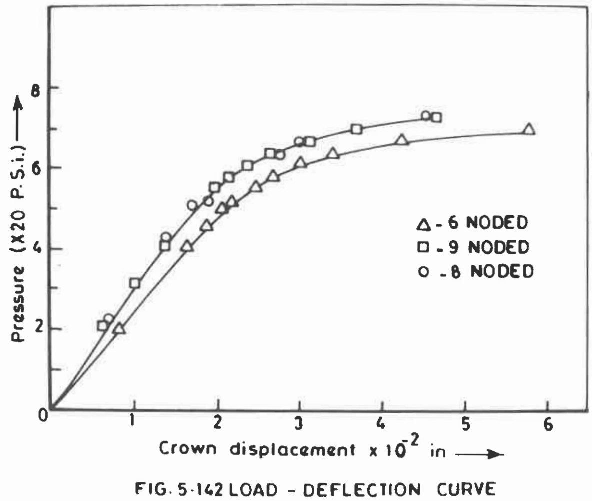

Fig. 12

Table 1.

Number of nodes per element	Number of elements	Number of nodal points	Number of degrees of freedom	Maximum aspect ratio
4	74	150	288	4.75
8	37	188	358	9.5
9	37	225	432	9.5
6	10	42	72	75.0

6 noded element gives values of deflection slightly in excess of those obtained with 8 and 9 noded elements (Fig. 12). This is because of the modified elasticity matrix which makes the structure flexible.

The results of the parametric studies done with different radius/thickness ratios clearly demonstrate the versatility of the 6 noded paralinear element as regards its ability to model thin/moderately thick axisymmetric structures. The use of the complicated shell theory is totally dispensed-with and in the case of thin elements the use of the differential displacements and the modified elasticity matrix makes it possible to analyse the structure with very few degrees of freedom, bringing down the CPU time and the core memory requirements. Its advantage is particularly evident in the non-linear analyses where the stiffness matrix has to be assembled and the solution has to be done a large number of times.

REFFRENCES

Abel, J.F. & S.T. Wu. 1979. Experience with a new triangular doubly curved element for shell analysis. Trans. SMiRT-5. vol.M. Paper M5/3.

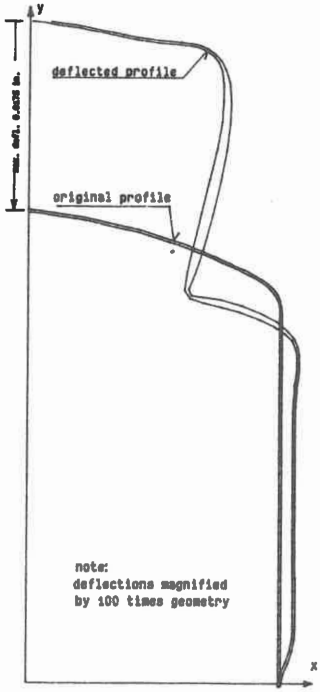

Fig. 13

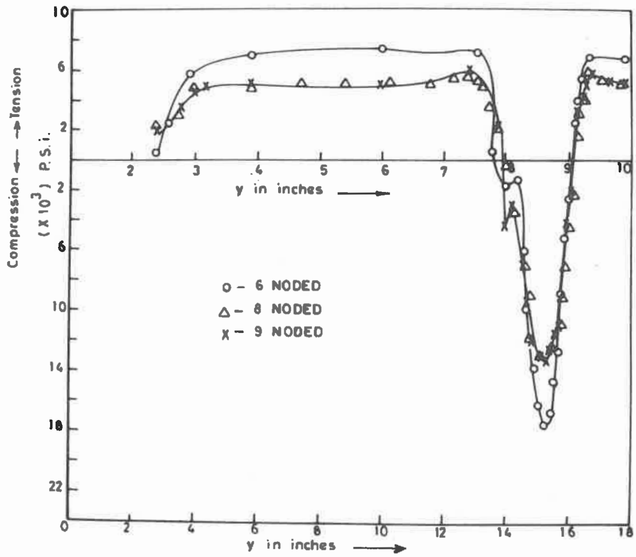

Fig. 14

Baluch, M.H. 1970. Analysis of stresses and deformations in moderately thick shells. Ph.D. Thesis, Purdue University, West Lafyette, Indiana.

Clauss, D.B. & D.S. Morschel. 1985. Comparison of analytical and experimental results from pressurisation of 1:8 scale steel containment model. Trans. SMiRT-8. vol.J. Paper J2/5.

Daye, M.A. & B.L. Mayers. 1985. Evaluation BWR and PWR containment structures subjected to internal pressure. Trans, SMiRT-8. vol.J. Paper 1/4.

Goldberg, J.E., Y.K. Tang, M.H. Baluch. & D.V. Pathak. 1975. Analysis of moderately thick shells of revolution. J. of Structural Engineering Division. ASCE. Proc. 101:821-838.

Kant, T. 1976. Thick shells of revolution - some studies. Ph.D. Thesis. Indian Institute of Technology, Bombay.

Khatua, T.P. & A. Al Dabbagh . 1979. Nonlinear finite element analysis of RC structures subjected to thermal load. Trans. SMiRT-5. vol.M. Paper M2/8.

Larkin, P.A., R.E. Stoner, R.L. Back & T.F. Huang. 1979. Mathematical modelling of a Mark III/BWR-6 containment for LOCA and SRV analysis. Trans. SMiRT-5. vol.J. Paper J2/9.

Mc Gaughy, J.P., F.T. Lin & S.K. Sen. 1983. Ultimate internal pressure carrying capacity of a reinforced concrete Mark III containment. Trans. SMiRT-6. vol.J. Paper J9/8.

Rashid, Y.R. & W. Rockenhauser. 1968. Pressure vessel analysis by finite element techniques. Conf. on Prestressed Concrete Vessels. Inst. of Civil Engineers. 38:385-434.

Sharma, S., M. Reich. & T.Y. Chang. 1983. Nonlinear finite element analysis of reinforced concrete Mark III containment under pressure and gravity loads. Trans. SMiRT-7. vol.M. Paper M2/8.

Steele, C.R., C.V. Ranjan, C. Goto. & T.H. Pulliam. 1979. FAST-A shell code using asymptotic results. Trans. SMiRT-5. vol.M. Paper M4/3.

Takeda, H. & W. Imoto. 1975. Inelastic analysis of multicavity PCRV under internal pressure. Trans. SMiRT-3. vol.H. Paper H2/5.

Timoshenko, S. & S.W. Krieger. 1970. Theory of Plates and Shells. McGraw-Hill, New York. 474-477.

Wade, M.T. & W. Henrywood. 1975. Experience in the application of finite element system to the analysis of complex prestressed concrete pressure vessels. Trans. SMiRT-3. vol.H. Paper H2/3.

Yamaura, Y., S. Igarashi, D.Z.F. Deng. & M. Tsay. 1985. Pressure capacity of a cylindrical steel containment vessel. Trans. SMiRT-8, vol.J. Paper J2/7.

Zudans, Z. 1970. Finite element incremental elastic plastic analysis of pressure vessels. J. of Engineering for Industry. ASME. 92:293-301.